0090-9556/08/3611-2171–2184$20.00
DRUG METABOLISM AND DISPOSITION
Vol. 36, No. 11
21956/3398670
Printed in U.S.A.

DMD 36:2171–2184, 2008

Identification of Stereoisomeric Metabolites of Meisoindigo in Rat Liver Microsomes by Achiral and Chiral Liquid Chromatography/Tandem Mass Spectrometry

Meng Huang, Lin Tang Goh, and Paul C. Ho

Department of Pharmacy, Faculty of Science, National University of Singapore, Singapore (M.H., P.C.H.); and Market Development and Applications, Waters Asia Headquarters, Waters Asia Limited, Singapore (L.T.G.)

Received April 21, 2008; accepted August 15, 2008

ABSTRACT:

***N*-Methylisoindigotin, abbreviated as meisoindigo, has been a routine therapeutic agent in the clinical treatment of chronic myelogenous leukemia in China since the 1980s. However, information relevant to in vitro metabolism of meisoindigo is limited. In this study, in vitro stereoisomeric metabolites of meisoindigo in rat liver microsomes were identified for the first time by achiral and chiral liquid chromatography/tandem mass spectrometry, together with proton NMR spectroscopy and synchrotron infrared spectroscopy. The major in vitro phase I metabolites of meisoindigo were tentatively identified as stereoselective-reduced meisoindigo, which comprised a pair of (3-*R*, 3′-*R*) and (3-*S*, 3′-*S*) enantiomers with lower abundance, as well as another pair of (3-*R*, 3′-*S*) and (3-*S*, 3′-*R*) enantiomers with higher abundance. One type of minor in vitro metabolites was tentatively identified as stereoselective *N*-demethyl-reduced meisoindigo including a pair of (3-*R*, 3′-*R*) and (3-*S*, 3′-*S*) enantiomers, as well as one meso compound. Another type of minor in vitro metabolites was tentatively identified as both stereoselective and regioselective monohydroxyl-reduced meisoindigo. Based on the metabolite profiling, three parallel metabolic pathways of meisoindigo in rat liver microsomes were proposed.**

Meisoindigo [3-(1,2-dihydro-2-oxo-3*H*-indol-3-ylidene)-1,3-dihydro-1-methyl-2*H*-indol-2-one], a synthetic derivative of indirubin from a traditional Chinese medicine recipe, has been a routine therapeutic agent in the clinical treatment of chronic myelogenous leukemia (CML) in China since the 1980s (Cooperative Group of Clinical Therapy of Meisoindigo, 1988; Xiao et al., 2000, 2002). A recent study indicated that the antiangiogenesis effect of meisoindigo may contribute to the antileukemic effect of this drug (Xiao et al., 2006). Meisoindigo was equally efficient for both treated and previously treated CML patients. The hematological complete response and partial response rates were 45.0 and 39.3% for newly diagnosed patients and 35.9 and 41.4% for pretreated patients (Cooperative Group of Phase III Clinical Trial on Meisoindigo, 1997). In addition, based on retrospective analysis on the efficiency of different treatments for 274 CML patients followed over a period of 5 years, meisoindigo in combination with hydroxyurea significantly prolonged median duration of chronic phase and median survival, as well as reduced incidence of blast crisis compared with meisoindigo or hydroxyurea alone, which strongly indicated that meisoindigo has a synergistic effect with hydroxyurea (Liu et al., 2000; Xiao et al., 2000). Meisoindigo was generally well tolerated. The most frequent side effects were bone, joint, and/or muscle pain of varying degrees when the dosage was more than the suitable dose. Approximately 30% of patients had mild nausea and vomiting (Cooperative Group of Clinical Therapy of Meisoindigo, 1988; Cooperative Group of Phase III Clinical Trial on Meisoindigo, 1997; Liu et al., 2000; Xiao et al., 2000).

To improve the understanding of its efficacy and safety characteristics, investigation of meisoindigo metabolism in animals or humans plays a critical role. However, few publications relevant to this topic have been reported so far. According to the literature survey information, only one individual study was highly relevant to meisoindigo metabolism (Peng and Wang, 1990). In that study, in vitro metabolism of meisoindigo in male rat liver microsomes was investigated by reversed-phase/high-performance liquid chromatography (HPLC) with diode array detector. Based on the UV chromatogram comparison of control and sample with parallel preparation, it was proposed that 10 chromatographic peaks were potential in vitro metabolites of meisoindigo. Among them, two major chromatographic peaks were purified by preparative thin-layer chromatography and predicted to be monohydroxy metabolites based on preliminary electron impact mass spectrometry (MS) results. However, there are a few severe draw-

Article, publication date, and citation information can be found at http://dmd.aspetjournals.org.
doi:10.1124/dmd.108.021956.

ABBREVIATIONS: CML, chronic myelogenous leukemia; HPLC, high-performance liquid chromatography; MS, mass spectrometry; LC, liquid chromatography; MS/MS, tandem mass spectrometry; IR, infrared; DMSO, dimethyl sulfoxide; QTRAP, hybrid triple quadrupole linear ion trap; CUR, curtain gas; GS1, ion source gas 1; GS2, ion source gas 2; TEM, source temperature; DP, declustering potential; CE, collision energy; EP, entrance potential; EMS, enhanced Q3 single MS; EPI, enhanced product ion; UPLC, ultra performance liquid chromatography; TIC, total ion chromatogram; QTOF, hybrid quadrupole time of flight; MRM, multiple reaction monitoring; XIC, extracted ion chromatogram; P450, cytochrome P450; NOE, nuclear Overhauser effect; MS/MS/MS, tandem mass spectra.

backs with regard to its experimental design. The substrate concentration adopted in that study far exceeded the upper limit of the typical concentration range (10–50 μM) in metabolite identification experiments (Chen et al., 2007). In addition, liquid-liquid extraction performed in that study was likely to cause the metabolites loss (Clarke et al., 2001) because physicochemical properties of metabolites present are unknown in a certain extraction solvent or a mixed extraction solvent system. Therefore, in vitro metabolism of meisoindigo in male rat liver microsomes still needs to be investigated with an appropriate experimental design.

Diverse bioanalytical technologies have been applied in the field of drug metabolism, such as radioimmunoassay, gas chromatography/MS, liquid chromatography (LC) with UV, fluorescence, radioactivity, and tandem mass spectrometry (MS/MS). Among these technologies, LC coupled with tandem MS (LC/MS/MS) has now become the most powerful tool owing to its superior specificity, sensitivity, and efficiency (Kostiainen et al., 2003). However, LC/MS/MS alone does not always provide sufficient information for structural characterization of metabolites, particularly in the aspects of identifying the exact position of oxidation, differentiating isomers, or providing the precise structure of unusual and/or unstable metabolites (Prakash et al., 2007). In these cases, other analytical technologies such as NMR, infrared (IR), or even chiral chromatography analysis have to be used to supplement additional information. In light of these considerations mentioned above, the purpose of the present study was to qualitatively identify the in vitro metabolites of meisoindigo in rat liver microsomes using online LC/MS/MS and other relevant techniques if necessary.

Materials and Methods

Chemicals. All the chemicals were of analytical grade and used without further purification. Meisoindigo was provided by Institute of Materia Medica, Chinese Academy of Medical Sciences, and Peking Union Medical College, Beijing, China. Bradford reagent, bovine serum albumin, β-NADPH, dimethyl sulfoxide (DMSO), ammonium acetate, palladium on carbon, and deuterochloroform were purchased from Sigma-Aldrich (St. Louis, MO). HPLC-grade methanol and acetonitrile were purchased from Thermo Fisher Scientific (Waltham, MA). Milli-Q water was obtained from a Millipore Corporation (Billerica, MA) water purification system and used to prepare buffer solutions and other aqueous solutions.

Liver Microsomal Preparation. Pooled rat liver microsomes were prepared according to the method reported previously (Gibson and Skett, 1994). Male Sprague-Dawley rats were obtained from Animal Holding Unit, National University of Singapore. Three rats were euthanized with CO_2 after a 24-h fasting period. The pooled extracted liver microsomes were suspended in 0.1 M Tris buffer, pH 7.4, and stored at −80°C before use. The microsomal protein contents were determined by the Bradford assay method, using bovine serum albumin as the standard protein (Bradford, 1976).

Liver Microsomal Incubations. Meisoindigo stock solution in DMSO was added to 0.1 M Tris buffer, pH 7.4, with rat liver microsomes. The mixture was first shaken for 5 min for equilibration in a shaking water bath at 37°C. The incubation was then initiated by adding β-NADPH solution. The final concentrations of meisoindigo, NADPH, and the microsomal protein were 50 μM, 1 mM, and 1 mg/ml, respectively, in a typical incubation mixture (1 ml). The percentage of DMSO in the incubation mixture was kept less than 0.2% (v/v). Controls were prepared either by substituting microsomal protein previously heated to 70 to 100°C for 10 min or by replacing NAPDH with water. Samples were incubated for 60 min, and the reaction was terminated with the same volume of ice-cold acetonitrile to precipitate proteins. Samples were subsequently centrifuged at 14,000 rpm for 15 min. The supernatant was taken and analyzed by LC/MS/MS. All the experiments were carried out in duplicate.

Achiral LC/MS/MS Analysis. *HPLC/hybrid triple quadrupole linear ion trap.* Five microliters of controls and samples were analyzed on a hybrid triple quadrupole linear ion trap (QTRAP) 2000 LC/MS/MS system from Applied Biosystems/MDS Sciex (Concord, ON, Canada) coupled to an Agilent 1100 HPLC system (Agilent Technologies, Palo Alto, CA). Separations were accomplished on an Agilent Hypersil ODS column (100 × 2.1 mm, 5 μm) (Agilent Technologies) with a guard cartridge at ambient temperature of about 22°C. The mobile phase consisted of 10 mM ammonium acetate in water (solvent A) and methanol (solvent B) and was delivered at a flow rate of 0.2 ml/min. The linear gradient elution program was as follows: 30 to 100% B over 12 min, followed by an isocratic hold at 100% B for another 3 min. At 15 min, B was returned to 30% in 1 min, and the column was equilibrated for 19 min before the next injection. The total run time was 35 min. During LC/MS/MS analysis, up to 3 min of the initial flow was diverted away from the mass spectrometer before evaluation of metabolites. The mass spectrometer was operated in the positive ion mode with a TurboIonSpray source. The parameter conditions were optimized as follows: curtain gas (CUR), 30 (arbitrary units); ion source gas 1 (GS1), 50 (arbitrary units); ion source gas 2 (GS2), 60 (arbitrary units); source temperature (TEM), 300°C; declustering potential (DP), 26 V; collision energy (CE), 35 eV; and entrance potential (EP), 4.5 V. Enhanced Q3 single MS (EMS) and enhanced product ion (EPI) were used to obtain structural information of the metabolites. The MS full-scan range was set to *m/z* 50 to 350. The mass spectrometer and the HPLC system were controlled by Analyst 1.4.1 software from Applied Biosystems/MDS Sciex.

Ultra performance LC/hybrid quadrupole time of flight. Accurate mass spectral data for the metabolites were obtained with a Q-TOF Premier mass spectrometer (Waters Micromass, Manchester, UK) coupled to an ACQUITY ultra performance LC (UPLC) system (Waters, Milford, MA). The separations were performed on an ACQUITY UPLC BEH C18 column (100 × 2.1 mm, 1.7 μm). The column was maintained at 40°C and eluted with a mobile phase consisting of 0.1% formic acid in water (solvent A) and 0.1% formic acid in methanol (solvent B) at 0.4 ml/min. The gradient elution program was as follows: 30 to 95% B over 6 min, followed by increasing to 99% B over 0.1 min. Then B was returned to 30% in 0.1 min, and the column was equilibrated for 1.8 min before the next injection. The total run time was 8 min. The autosampler chamber was maintained at 10°C, and the injection volume was 4 μl. The column eluent was directed to the mass spectrometer for analysis. The mass spectrometer was equipped with an electrospray ionization source and operated in the positive ionization mode. Full-scan spectra were acquired from 50 to 1000 *m/z* with a scan time of 0.3 s. The capillary and cone voltages were 3.0 kV and 25 V, respectively. The source and desolvation temperatures were 90 and 180°C, respectively. The desolvation gas flow rate was 400 l/h, and the cone gas flow rate was 10 l/h. The collision energy was set at 4 eV. All the analyses were acquired using an independent reference spray via the LockSpray interference to ensure accuracy and reproducibility. The $[M+H]^+$ ion of sulfadimethoxine was used as the lock mass (*m/z* 311.0814). The LockSpray frequency was set at 15 s. The accurate masses and compositions for the precursor ions were calculated using the MassLynx version 4.0 software (Waters) incorporated in the instrument.

Search for metabolites. The total ion chromatograms (TICs) of controls and samples for the EMS were first compared. The search for structure-related metabolites of meisoindigo was performed manually by interpretation of mass spectra and chromatograms. The possible molecular masses of metabolites were screened out based on known mass shift of metabolites such as +16 for hydroxylation. The corresponding EPI (MS/MS) of potential metabolites was subsequently compared with that of meisoindigo to investigate the fragmentation patterns and obtain information on the metabolite structures. Besides, MS/MS/MS of certain product ions gave more evidence about the deduction of fragmentation mechanism. Hybrid quadrupole time of flight (QTOF) data also provided the accurate masses and potential formulae to further confirm the structures of metabolites.

Isolation of metabolites by preparative HPLC and MS/MS/MS. The major metabolites were isolated from a large-scale phenobarbital-induced rat liver microsomal incubation by Agilent 1100 preparative HPLC system (Agilent Technologies) on a Combi-A C18 column (50 × 20 mm, 5 μm) (Peeke Scientific, Redwood City, CA) with a guard cartridge at ambient temperature. The mobile phase consisted of water (solvent A) and methanol (solvent B) and was delivered at a flow rate of 4 ml/min. The linear gradient elution program was as follows: 30% to 100% B over 20 min, followed by an isocratic hold at 100% B for another 5 min. At 25 min, B was returned to 30% in 1 min, and the column was equilibrated for 4 min before the next manual injection. The UV absorbance was monitored at 254 nm. All the isolated metabolite fractions

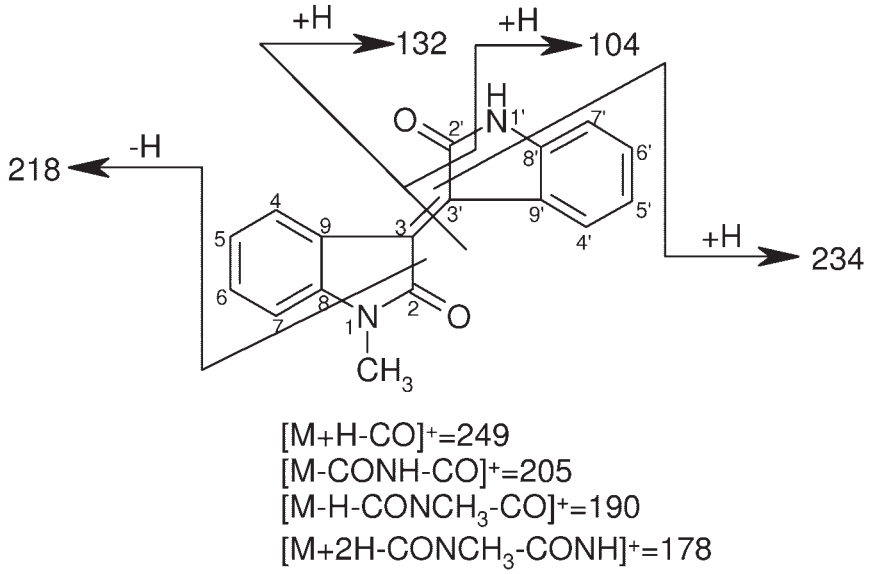

$[M+H-CO]^+=249$
$[M-CONH-CO]^+=205$
$[M-H-CONCH_3-CO]^+=190$
$[M+2H-CONCH_3-CONH]^+=178$

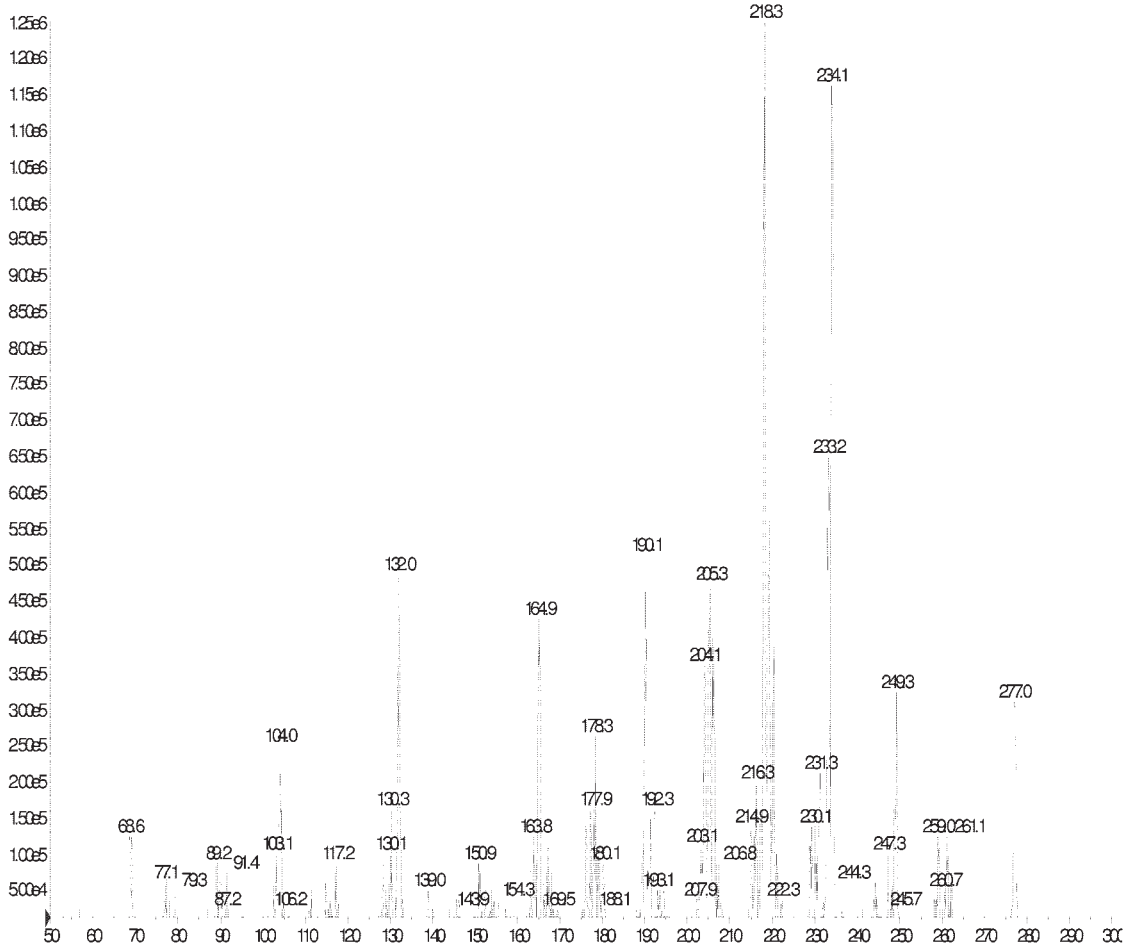

FIG. 1. MS/MS spectrum of protonated meisoindigo at *m/z* 277 and the proposed origin of key product ions.

were lyophilized and redissolved in 50% methanol/water before chiral separation or direct infusion for MS/MS/MS analysis.

Chiral LC/MS/MS Analysis. The rat liver microsomal samples and isolated metabolite fractions were analyzed on a QTRAP 3200 LC/MS/MS system from Applied Biosystems/MDS Sciex coupled to an Agilent 1200 HPLC system (Agilent Technologies). The volume of 20 μl was injected onto a Chiralcel OD-R column (250 $\times$ 4.6 mm, 10 μm) (Daicel Chemical Industries, Ltd., Osaka, Japan) with a guard cartridge at ambient temperature. The isocratic mobile phase consisted of 20% water (solvent A) and 80% methanol (solvent B) and was delivered at a flow rate of 0.4 ml/min. The total run time was 35 min. The mass spectrometer was operated in the positive ion mode with a TurboIonSpray source. The parameter conditions were optimized as follows:

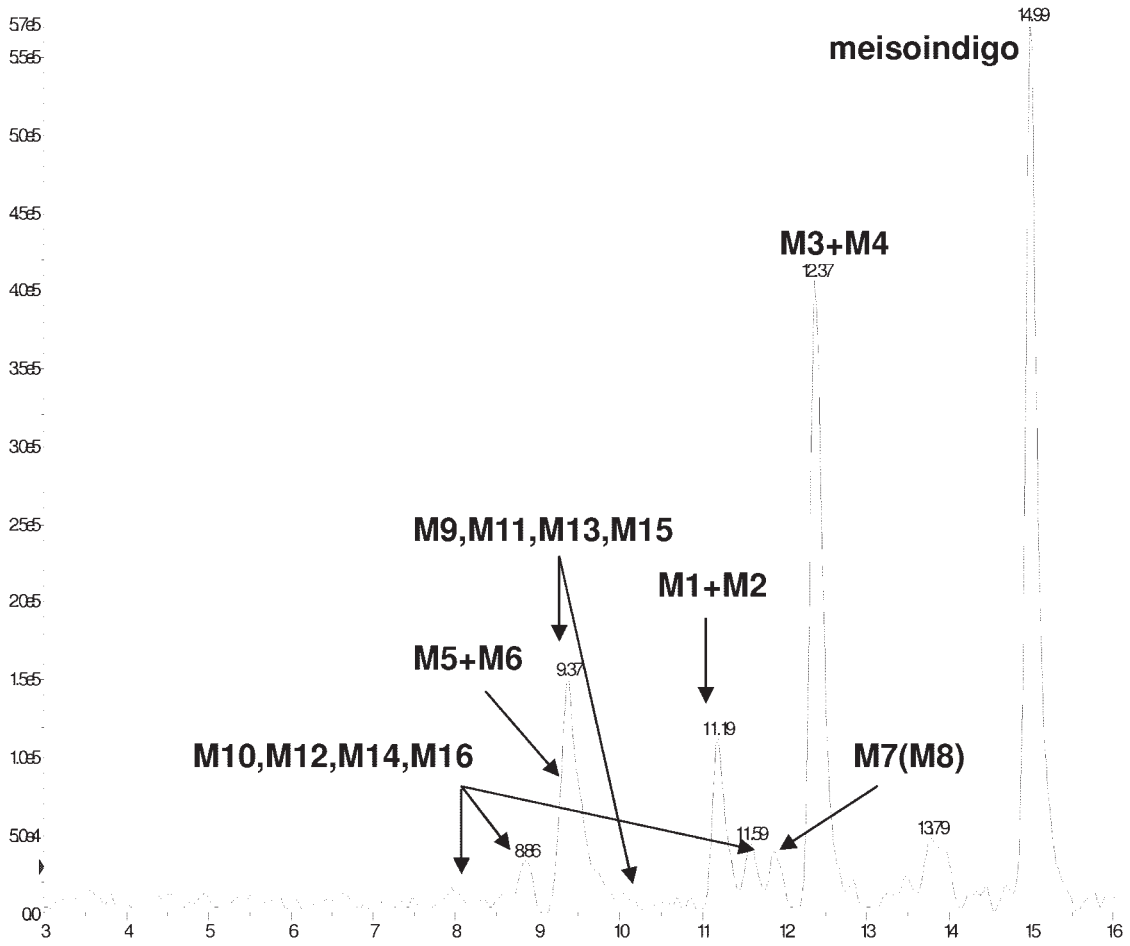

FIG. 2. Reconstructed extract ion chromatogram for meisoindigo and its metabolites in rat liver microsomes.

TABLE 1

HPLC/QTAP retention times and mass spectra properties for meisoindigo and its in vitro metabolites

	Retention Time	MH^+	*m/z* of Major Product Ions
	min		
Meisoindigo	14.99	277	249,234,218,205,190,178,165,132,104
M1 + M2	11.19	279	261,251,234,223,147,133,118
M3 + M4	12.37		
M5 + M6	9.30	265	247,237,219,209,133
M7 (M8)	11.87		
M9, M11, M13, M15	9.37, 10.34	295	277,267,251,163,134,133
M10, M12, M14, M16	7.97, 8.86, 11.59		277,267,249,158,149,147

CUR, 20 (arbitrary units); GS1, 30 (arbitrary units); GS2, 40 (arbitrary units); TEM, 450°C; DP, 35 V; CE, 30 eV; and EP, 10 V. EMS was used to scan the mass range of m/*z* 50 to 700. The mass spectrometer and the HPLC system were controlled by Analyst 1.4.2 software from Applied Biosystems/MDS Sciex.

Metabolite synthesis and purification. The starting material meisoindigo (50 mg) was dissolved in methanol (100 ml). After adding 10% palladium on carbon (10 mg), the mixture was placed on the hydrogenator apparatus and kept shaking at 40 psi for 2 h at room temperature. LC/MS was used to monitor the consumption of starting material. The reaction mixture was filtered through filter paper, and the filter pad was washed with distilled water. The filtrate was evaporated under reduced pressure, and the precipitate was purified by the same preparative HPLC and column described above. The isocratic mobile phase consisted of 50% water (solvent A) and 50% methanol (solvent B) and was delivered at a flow rate of 4 ml/min within 20 min. The UV absorbance was monitored at 254 nm. All the isolated metabolite fractions were evaporated under reduced pressure and stored under −20°C before NMR measurement.

NMR spectroscopy. Proton NMR spectra of synthesized metabolites were recorded in deuterochloroform at room temperature on a Bruker DRX 500 MHz NMR spectrometer (Bruker, Newark, DE) using tetramethylsilane as an internal standard.

Synchrotron IR spectroscopy. IR spectra were recorded through grazing incidence angle in reflection mode on a Bruker IFS 66v/S Fourier Transform IR spectrometer (Bruker) with a synchrotron light source. The IR spectral range was from approximately 650/cm to 4000/cm with a resolution of 4/cm. A KBr beamsplitter and mid-band MCT IR detector cooled to 77 K were used. The samples were dissolved in acetonitrile and subsequently coated on gold substrate after solvent evaporation. Spectra of thin film of samples on gold are directly acquired in the vacuum.

Comparative Study on Incubations under Normoxic and Hypoxic Conditions. In normoxic incubation, meisoindigo stock solution in methanol was added to 0.1 M Tris buffer, pH 7.4, with rat liver microsomes. The mixture was first shaken for 5 min for equilibration in a shaking water bath at 37°C. The incubation was then initiated by adding β-NADPH solution. The final con-

TABLE 2

UPLC/QTOF retention times, potential formula, and accurate masses for meisoindigo and its in vitro metabolites

	Retention Time	Molecular Formula (1+)	*m/z* (1+)	Del M	Measured *m/z* (1+)	PPM
	min			*Da*		
Meisoindigo	3.42	$C_{17}H_{13}N_2O_2$	277.0977	−0.0001	277.0976	−0.4
M1 + M2	2.07	$C_{17}H_{15}N_2O_2$	279.1134	2.0162	279.1139	1.8
M3 + M4	2.43			2.0153	279.1130	−1.4
M5 + M6	1.65	$C_{16}H_{13}N_2O_2$	265.0977	−12.0005	265.0972	−1.9
M7 (M8)	2.26			−11.9996	265.0981	1.5
M9, M11, M13, M15	1.66	$C_{17}H_{15}N_2O_3$	295.1083	18.0104	295.1081	−0.7
	1.74			18.0111	295.1088	1.7
M10, M12, M14, M16	1.45			18.0111	295.1088	1.7
	1.56			18.0113	295.1090	2.4
	2.17			18.0101	295.1078	−1.7

centrations of meisoindigo, NADPH, and the microsomal protein were 10 μM, 1 mM, and 1 mg/ml, respectively, in a typical incubation mixture (1 ml). The percentage of methanol in the incubation mixture was kept less than 1% (v/v). Aliquots of 100 μl of the incubation sample mixtures were collected at 5, 15, 30, and 60 min, and the reaction was terminated with the same volume of ice-cold acetonitrile to precipitate proteins. Samples were subsequently centrifuged at 14,000 rpm for 15 min. Five microliters of the supernatant was taken and analyzed by LC/MS/MS. In hypoxic incubation, meisoindigo and rat liver microsomes were preincubated at 37°C and bubbled with 100% nitrogen gas (the tip of the nitrogen gas supply was submerged approximately 2 mm in the solution) for 5 min. The incubation was then initiated by adding β-NADPH solution. The rest of the procedures for sample collection and preparation was the same as described above except the continuous nitrogen gas supply throughout the study. Negative controls were prepared either by substituting microsomal protein previously heated to 70 to 100°C for 10 min or by replacing NAPDH with water under both normoxic and hypoxic conditions.

The analysis was conducted on a QTRAP 3200 MS/MS system from Applied Biosystems/MDS Sciex coupled to an Agilent 1200 HPLC system (Agilent Technologies). Separations were accomplished on a Luna C18 column (150 × 2.0 mm, 5 μm) (Phenomenex, Torrance, CA) with a guard cartridge at ambient temperature. The mobile phase consisted of 0.1% formic acid in water (solvent A) and acetonitrile (solvent B) and was delivered at a flow rate of 0.2 ml/min. The linear gradient elution program was as follows: 30% to 95% B over 13 min, followed by an isocratic hold at 95% B for another 7 min. At 20 min, B was returned to 30% in 1 min, and the column was equilibrated for 19 min before the next injection. The total run time for each injection was 40 min. The mass spectrometer was operated in the positive ion mode with a TurboIonSpray source. Two multiple reaction monitoring (MRM) transitions, i.e., 277.1→234.2 and 279.1→147.1, were used to determine meisoindigo and its metabolites at *m/z* 279, respectively. The DP and CE values were 66 V and 45 eV for meisoindigo and 61 V and 30 eV for the metabolites. The other ionization parameters were as follows: CUR, 20 (arbitrary units); GS1, 40 (arbitrary units); GS2, 50 (arbitrary units); TEM, 650°C; and EP, 10 V. The dwell time of each MRM transition was 150 ms. The mass spectrometer and the HPLC system were controlled by Analyst 1.4.2 software from Applied Biosystems/MDS Sciex. The relative percentages of the components in incubations were estimated at different incubation time points based on the integrated peak areas of MRM chromatograms.

Results

The proposed fragmentation scheme and product ions of protonated meisoindigo (*m/z* 277) are shown in Fig. 1. It contains major product ions at *m/z* 249, 234, 218, 205, 190, 178, 132, and 104. Loss of CO (28 Da) following gain of one H generated the product ion at *m/z* 249. Loss of CONH (43 Da) following gain of one H generated the product ion at *m/z* 234. Loss of $CONCH_3$ (57 Da) following loss of one H generated the product ion at *m/z* 218. Loss of both CONH and CO generated the product ion at *m/z* 205. Loss of both $CONCH_3$ and CO following loss of one H generated the product ion at *m/z* 190, which was confirmed by MS/MS/MS (data not shown). Loss of both $CONCH_3$ and CONH following gain of two H generated the product ion at *m/z* 178, which was confirmed by MS/MS/MS (data not shown). Cleavage of the 3,3′ double bond of meisoindigo following gain of one H, and subsequent loss of CO at position 2′ following gain of one H, generated the product ions at *m/z* 132 and 104, respectively.

The reconstructed extracted ion chromatogram (XIC) from HPLC/QTRAP was shown in Fig. 2. It was found that the parent drug and its metabolites were detected as their protonated molecules. Meisoindigo was eluted at 14.99 min and showed a molecular ion (MH^+) at *m/z* 277. Several metabolites were observed and eluted earlier than meisoindigo, between 7 and 13 min. Those metabolite peaks formed corresponding to masses of *m/z* 279 (11.19, 12.37 min), *m/z* 265 (9.30, 11.87 min), and *m/z* 295 (7.97, 8.86, 9.37, 10.34, and 11.59 min) (summarized in Table 1). From the relative peak areas in Fig. 2, meisoindigo remained the largest component, whereas two peaks corresponding to *m/z* 279 and one peak corresponding to *m/z* 295 were regarded as the major metabolites. The chromatographic profiles of meisoindigo and its metabolites from UPLC/QTOF showed a significant similarity as that from HPLC/QTRAP (data not shown). Table 2 showed the accurate masses and potential molecular formulae provided by UPLC/QTOF.

Protonated Metabolites at *m/z* 279. Metabolites at *m/z* 279 had retention times of 11.19 and 12.37 min on the HPLC system, respectively, and showed 2 Da increase of molecular mass compared with parent drug, suggesting they could be direct reduction products or *N*-demethylation followed by mono-oxidation products. The corresponding potential formula of metabolites at *m/z* 279 based on their accurate masses was $C_{17}H_{15}N_2O_2$ (Table 2), thus confirming the occurrence of direct reduction. Taking the identical molecular formulae with different retention times into account, these two metabolites could be isomers.

Both of the EPI (MS/MS) mass spectra on metabolites at *m/z* 279 of 11.19 and 12.37 min were identical, indicating these two metabolites should be stereoisomers. The proposed fragmentation scheme and MS/MS spectrum of protonated metabolites at *m/z* 279 are shown in Fig. 3. Loss of H_2O (18 Da) generated the product ion at *m/z* 261. Loss of one or two CO generated the product ion at *m/z* 251 or *m/z* 223, which indicated that reduction had not occurred on either of the carbonyl groups. Loss of CONH generated the product ion at *m/z* 234. Cleavage of the 3,3′ bond generated the product ions at *m/z* 147 and *m/z* 133, which was 1 Da higher than the corresponding product ion of meisoindigo at *m/z* 132, thus indicating the presence of 3,3′ single bond. Subsequent loss of CO at position 2 after the cleavage of the 3,3′ bond generated the product ions at *m/z* 118, which was confirmed by MS/MS/MS (data not shown).

Because direct double-bond reduction caused the generation of two chiral carbon centers located in position 3 and 3′, four stereoisomers, i.e., M1, M2, M3, and M4, at *m/z* 279 could exist with possible

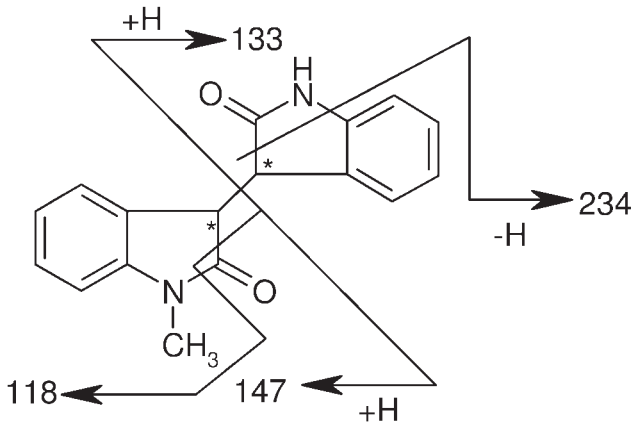

$[M+H-H_2O]^+=261$
$[M+H-CO]^+=251$
$[M+H-CO-CO]^+=223$

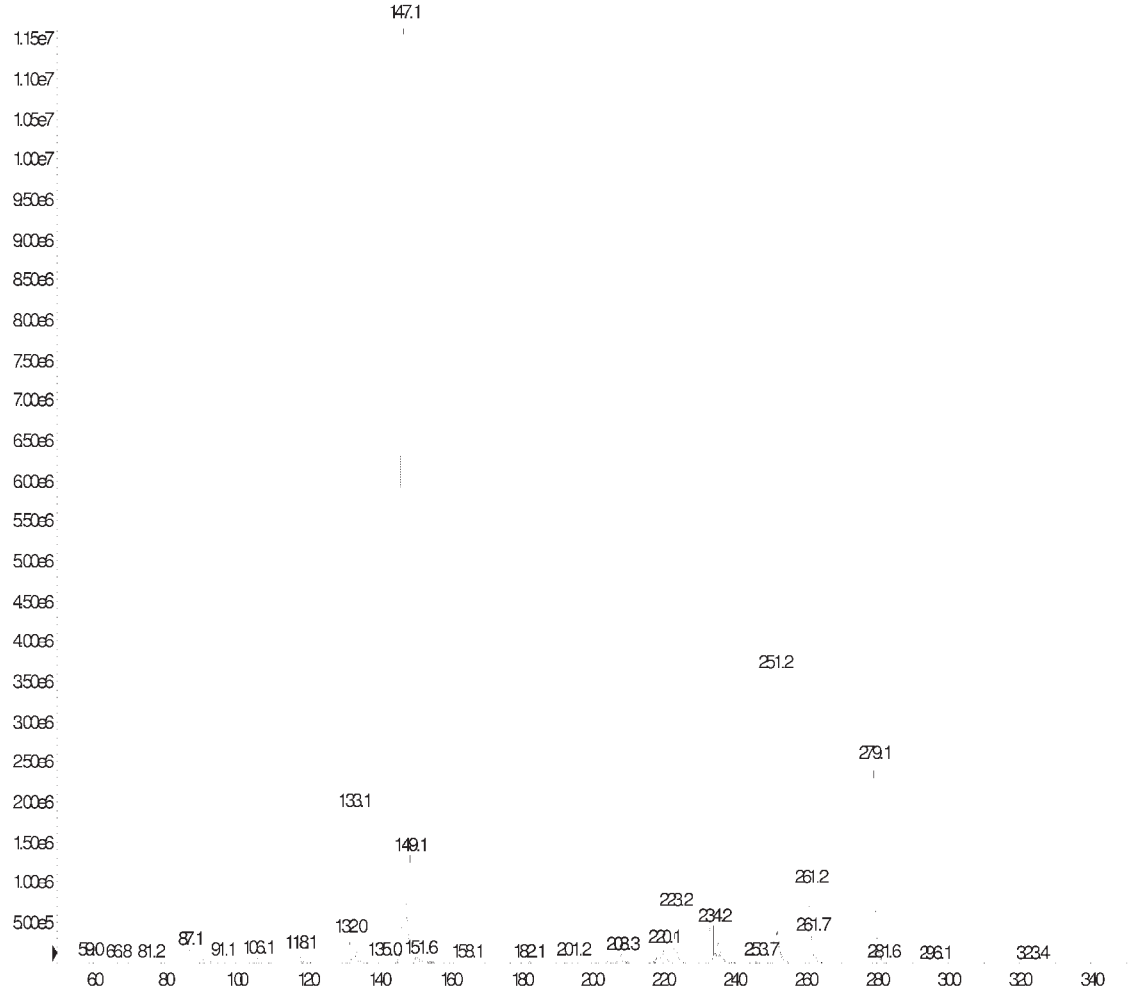

FIG. 3. MS/MS spectrum of protonated M1+M2, M3+M4 at *m/z* 279, and the proposed origin of key product ions.

absolute configurations of (3-*R*, 3′-*R*), (3-*S*, 3′-*S*), (3-*R*, 3′-*S*), and (3-*S*, 3′-*R*). Among them, M1 and M2, M3 and M4 were assumed as enantiomers of each other, respectively. In addition, M1 was diastereomer of M3 or M4. M2 was diastereomer of M3 or M4. Considering enantiomers generally show the same chromatographic properties with the use of nonchiral column whereas diastereomers seldom do, as well as only two peaks were displayed on the TIC or XIC, the peak with retention time of 11.19 min was postulated to be a combination of M1 and M2, whereas the other peak with retention time of 12.37 min was postulated to be a combination of M3 and M4.

The chromatographic behaviors of metabolites at *m/z* 279 on the chiral column further confirmed this postulation. The two peaks with

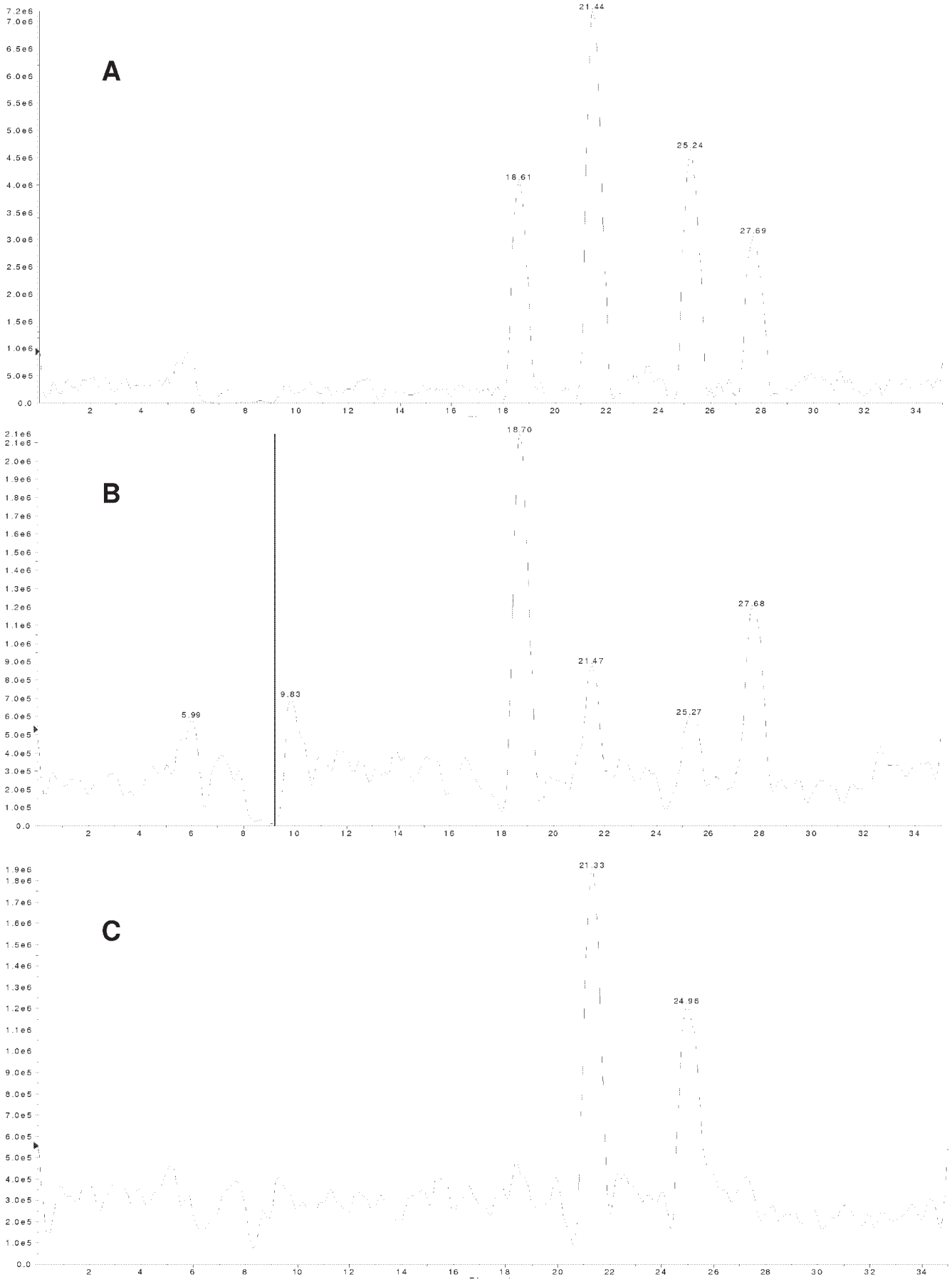

FIG. 4. Extracted ion chromatograms on the chiral column corresponding to M1+M2+M3+M4 (A), M1+M2 (B), and M3+M4 (C) at *m/z* 279.

TABLE 3

^{1}H NMR data for meisoindigo, M1 + M2, and M3 + M4

Position	Meisoindigo	M1 + M2	M3 + M4
4	9.13 (1H, d, 8.0 Hz)	7.26 (1H, t, 8.0 Hz)	7.23 (1H, t, 8.0 Hz)
5	7.08 (1H, m)	6.98 (1H, m)	6.95 (1H, m)
6	7.38 (1H, t, 7.5 Hz)	7.15 (1H, m)	7.12 (1H, m)
7	6.79 (1H, m)	6.74 (1H, m)	6.72 (1H, m)
4′	9.20 (1H, d, 8.0 Hz)	7.33 (1H, t, 8.0 Hz)	7.30 (1H, t, 8.0 Hz)
5′	7.05 (1H, m)	6.95 (1H, m)	6.92 (1H, m)
6′	7.32 (1H, t, 7.5 Hz)	7.08 (1H, t, 8.0 Hz)	7.05 (1H, t, 8.0 Hz)
7′	6.81 (1H, m)	6.81 (1H, t, 8.5 Hz)	6.78 (1H, m)
NCH_3	3.30 (3H, s)	3.17 (3H, s)	3.14 (3H, s)
NH	7.81 (1H, br.s)	7.58 (1H, br.s)	7.48 (1H, br.s)
3		4.23 (1H, dd, 3.5 Hz, 24.0 Hz)	4.20 (1H, dd, 3.5 Hz, 24.0 Hz)
3′		4.32 (1H, dd, 3.5 Hz, 26.0 Hz)	4.30 (1H, dd, 3.5 Hz, 27.0 Hz)

retention time of 11.19 and 12.37 min on the nonchiral column (Fig. 2) were split into four peaks on the chiral column, with retention times of 18.61, 21.44, 25.24, and 27.69 min, respectively (Fig. 4A). Interestingly, after separation of the two pairs of enantiomers through preparative HPLC, one pair of enantiomers (M1+M2) corresponded to the leftmost and rightmost peaks with the retention times of 18.70 and 27.68 min (Fig. 4B), whereas the other pair (M3+M4) corresponded to the two peaks in the middle with the retention times of 21.33 and 24.96 min (Fig. 4C), which suggested the chiral structure difference between M1 and M2 was larger than that between M3 and M4. Furthermore, the isolated pair of enantiomers (M1+M2) showed two additional small peaks happening to correspond to the other pair (M3+M4) (Fig. 4B), whereas the isolated (M3+M4) only showed two peaks (Fig. 4C), which strongly indicated that (M1+M2) was unstable, automatically converting to (M3+M4). Hence, the absolute configurations of (M1+M2) could be (3-*R*, 3′-*R*) and (3-*S*, 3′-*S*). Based on each stereoisomer's chromatographic peak areas shown in Fig. 4A, the reduction metabolism of meisoindigo was found to be stereoselective. One pair of enantiomers (M3+M4) showed a higher abundance than the other pair (M1+M2). Within both of these two pairs of enantiomers, the more polar stereoisomer eluted first was always of higher abundance than the less polar one (18.70 versus 27.68 min, 21.33 versus 24.96 min).

The hydrogenation of red meisoindigo generated colorless products in methanol solution. Diluted products showed the same retention times and fragmentation patterns on LC/MS/MS as the two metabolites at *m/z* 279 from microsomal sample. After isolation by preparative HPLC and solvent evaporation, two white solids of metabolites were obtained. The proton NMR signals of meisoindigo, M1+M2, and M3+M4 were assigned in Table 3, respectively. The significant similarity in proton NMR signals of M1+M2 and M3+M4 further confirmed the diastereomer relationship between them. Compared with the chemical shift values of meisoindigo, the chemical shift values of both M1+M2 and M3+M4 more or less shifted to relatively high field region because of the breakdown of long conjugation within the whole molecule caused by the forming of 3,3′ single bond. The synchrotron IR absorption spectra of two isolated metabolites at *m/z* 279 were very similar and shown in Fig. 8A. The broad band around 3200 to 3400/cm was assigned to be NH stretching vibration. The band around 2800 to 2900/cm was assigned to be CH_3 stretching vibration. The band around 1600/cm was assigned to be C = O stretching vibration. These characteristic absorption bands further confirmed the presence of NH, CH_3, and C = O.

Therefore, M1+M2 was tentatively identified as a pair of (3-*R*, 3′-*R*) and (3-*S*, 3′-*S*) reduced-meisoindigo enantiomers with two hydrogens located at the same side of 3,3′-single bond, whereas M3+M4 was another pair of (3-*R*, 3′-*S*) and (3-*S*, 3′-*R*) enantiomers with two hydrogens located at the opposite sides.

Protonated Metabolites at *m/z* 265. Metabolites at *m/z* 265 had retention times of 9.30 and 11.87 min on the HPLC system, respectively, and showed 12 Da decrease of molecular mass compared with parent drug, suggesting they could be direct reduction followed by *N*-demethylation products. The corresponding potential formula of metabolites at *m/z* 265 based on their accurate masses was $C_{16}H_{13}N_2O_2$ (Table 2), thus confirming this postulation. Taking the identical molecular formulae with different retention times into account, these two metabolites could be isomers.

Both of the EPI (MS/MS) mass spectra on metabolites at *m/z* 265 of 9.30 and 11.87 min were identical, indicating these two metabolites should be stereoisomers. The proposed fragmentation scheme and MS/MS spectrum of protonated metabolites at *m/z* 265 are shown in Fig. 5. Loss of H_2O generated the product ion at *m/z* 247, and subsequent loss of CO generated *m/z* 219. Loss of one or two CO generated the product ion at *m/z* 237 or *m/z* 209, which indicated that reduction had not occurred on either of the carbonyl groups. Cleavage of the 3,3′ bond generated the product ion at *m/z* 133 with the highest abundance, indicating the forming of a symmetric molecule after *N*-demethylation.

Because of the generation of two chiral carbon centers located in position 3 and 3′, four stereoisomers, i.e., M5, M6, M7, and M8, at *m/z* 265 could exist with possible absolute configuration of (3-*R*, 3′-*R*), (3-*S*, 3′-*S*), (3-*R*, 3′-*S*), and (3-*S*, 3′-*R*). Interestingly, reduction followed by *N*-demethylation led to the generation of the same segments on both sides of 3-3′ single bond. M5 (3-*R*, 3′-*R*) and M6 (3-*S*, 3′-*S*) were enantiomers of each other so that they were combined into one peak on the TIC or XIC with retention times of 9.30 min. However, M7 (3-*R*, 3′-*S*) and M8 (3-*S*, 3′-*R*) were actually the identical compound because of the presence of an internal symmetrical center at the midpoint of 3-3′ single bond. M7 (namely, M8) was a meso compound with retention times of 11.87 min. Furthermore, M7 (M8) exhibited a higher abundance than the pair of enantiomers (M5+M6) (Fig. 2), suggesting metabolites of *m/z* 265 also showed stereoselective metabolism in this case. Therefore, M5+M6 was tentatively identified as a pair of (3-*R*, 3′-*R*) and (3-*S*, 3′-*S*) *N*-demethyl reduced-meisoindigo enantiomers with two hydrogens located at the same side of 3,3′-single bond, whereas M7 (M8) was one meso compound with two hydrogens located at the opposite sides.

Protonated Metabolites at *m/z* 295. Metabolites at *m/z* 295 had retention times of 7.97, 8.86, 9.37, 10.34, and 11.59 min on the HPLC system, respectively, and showed 18 Da increase of molecular mass compared with parent drug, suggesting they could be direct reduction followed by mono-oxidation products. The corresponding potential formula of metabolites at *m/z* 295 based on their accurate masses was

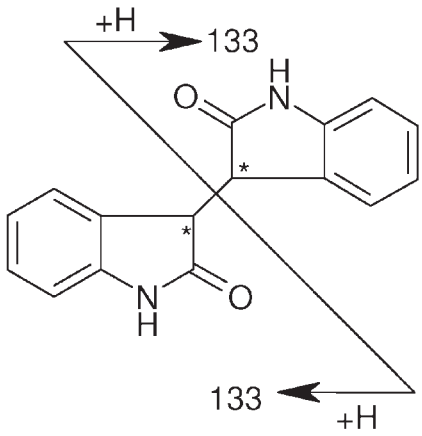

$[M+H-H_2O]^+=247$
$[M+H-CO]^+=237$
$[M+H-H_2O-CO]^+=219$
$[M+H-CO-CO]^+=209$

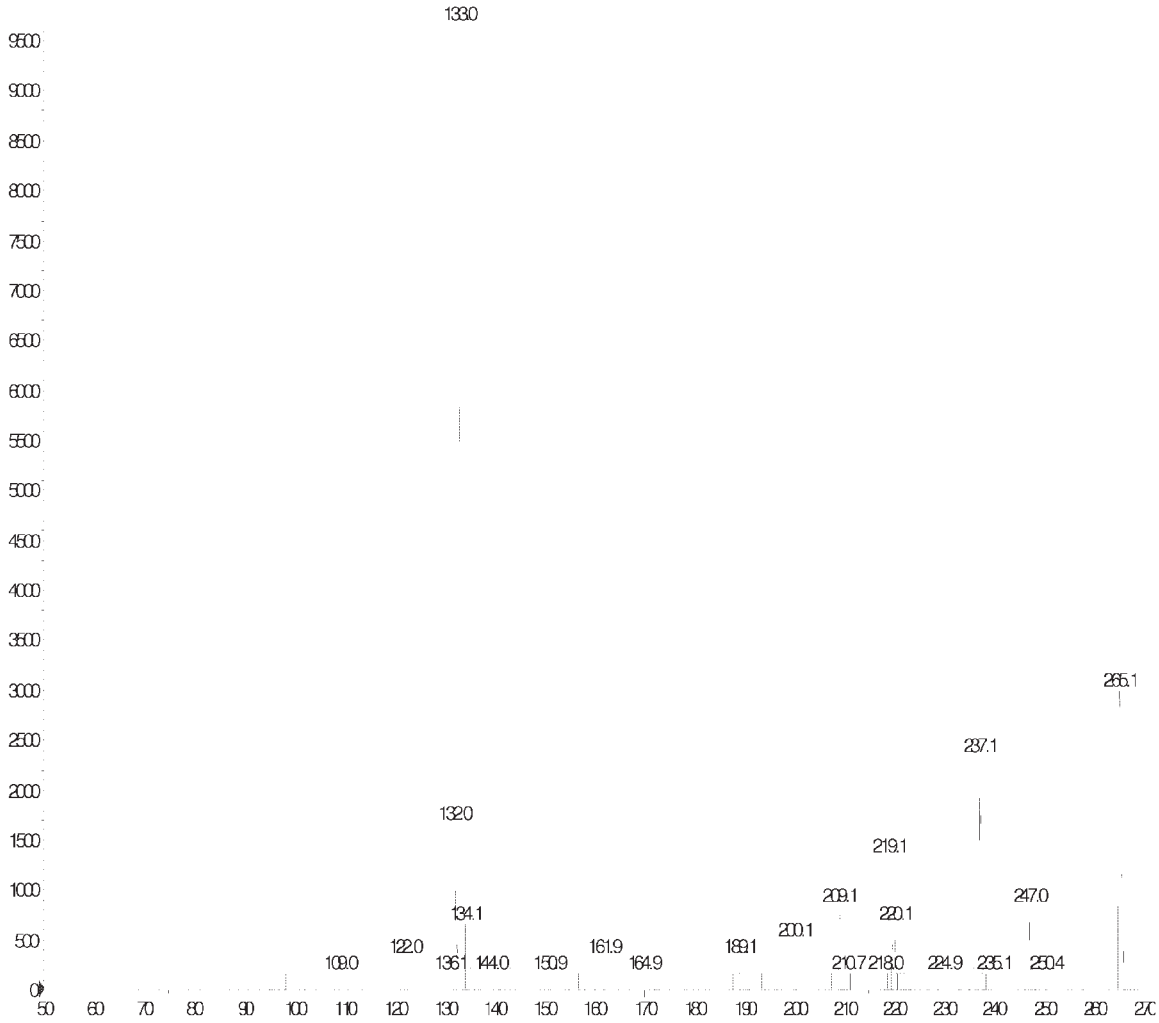

FIG. 5. MS/MS spectrum of protonated M5+M6, M7 (M8) at *m/z* 265, and the proposed origin of key product ions.

$C_{17}H_{15}N_2O_3$ (Table 2), thus confirming this postulation. Taking the identical molecular formulae with different retention times into account, these five metabolites could be isomers.

There were two types of EPI (MS/MS) mass spectra on metabolites at *m/z* 295. One type was the identical EPI of metabolites with retention times of 9.37 and 10.34 min, indicating these two metabo-

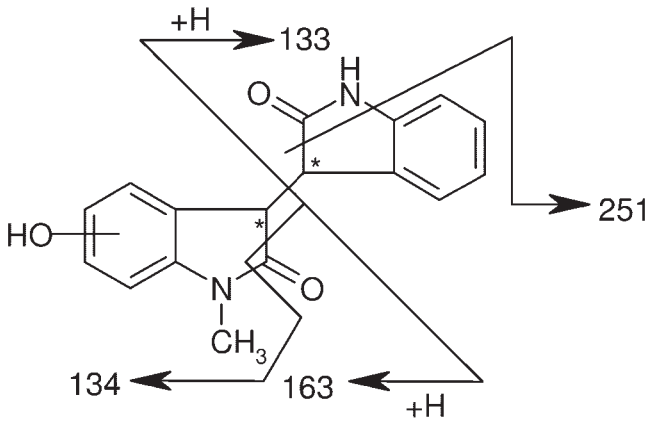

$[M+H-H_2O]^+=277$

$[M+H-CO]^+=267$

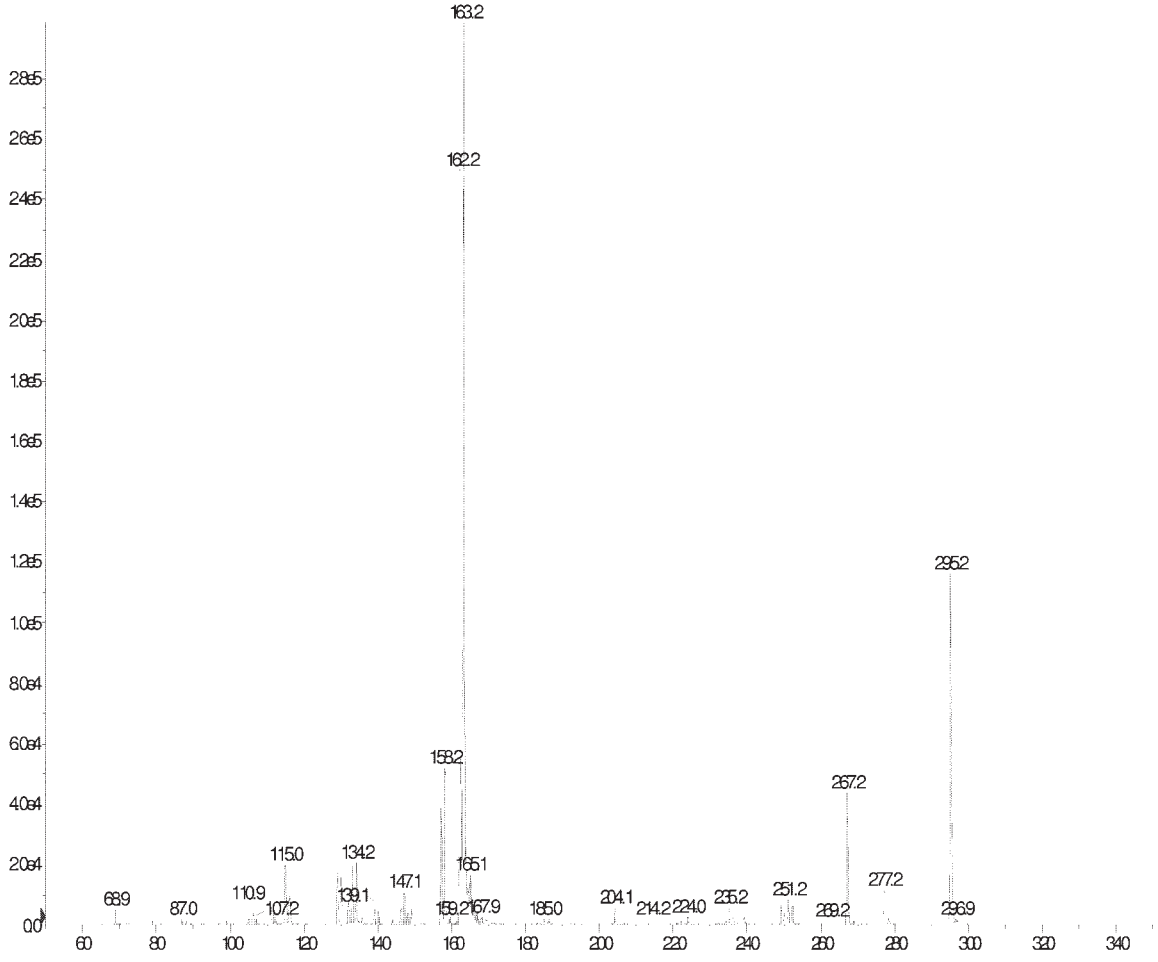

FIG. 6. MS/MS spectrum of protonated M9, M11, M13, and M15 at *m/z* 295 and the proposed origin of key product ions.

lites should be stereoisomers. The proposed fragmentation scheme and MS/MS spectrum of this type are shown in Fig. 6. Loss of H_2O generated the product ion at *m/z* 277. Loss of CO generated the product ion at *m/z* 267. Loss of CONH generated the product ion at *m/z* 251. Cleavage of the 3,3′ bond generated the product ions at *m/z* 163 and *m/z* 133, of which only *m/z* 163 was 16 Da higher than the corresponding product ion of reduced meisoindigo at *m/z* 147, thus indicating hydroxylation had occurred at one of the positions 4, 5, 6, and 7. Subsequent loss of CO at position 2 after the cleavage of the 3,3′ bond generated the product ions at *m/z* 134. The other type was the identical EPI of metabolites with retention times of 7.97, 8.86, and 11.59 min, indicating these three metabolites should be stereoisomers. The proposed fragmentation scheme and MS/MS spectrum of this type are shown in Fig. 7. Loss of both H_2O and CO generated the product ion at *m/z* 249. Cleavage of the 3,3′ bond generated the product ions at *m/z* 147 and *m/z* 149, of which only *m/z* 149 was 16

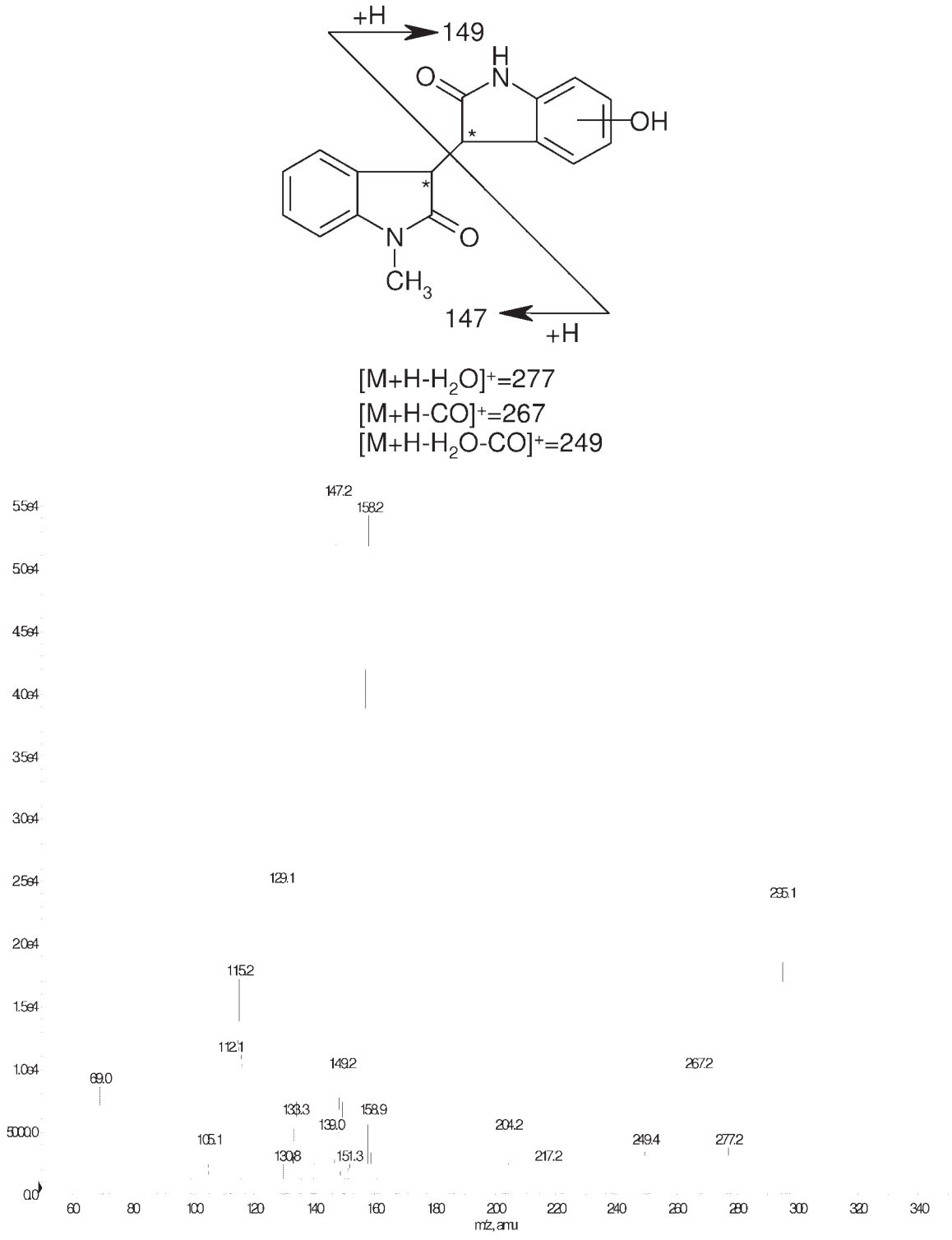

FIG. 7. MS/MS spectrum of protonated M10, M12, M14, and M16 at *m/z* 295 and the proposed origin of key product ions.

Da higher than the corresponding product ion of reduced meisoindigo at *m/z* 133, thus indicating hydroxylation had occurred at one of the positions 4′, 5′, 6′, and 7′.

Reduction followed by phenyl single oxidation led to two different types of position isomers. Considering the generation of two chiral carbon centers located in position 3 and 3′, the first type could involve M9 (3-*R*, 3′-*R*), M11 (3-*S*, 3′-*S*), M13 (3-*R*, 3′-*S*), M15 (3-*S*, 3′-*R*), with single hydroxyl group at position 4, 5, 6, or 7. The second type could involve M10 (3-*R*, 3′-*R*), M12 (3-*S*, 3′-*S*), M14 (3-*R*, 3′-*S*), M16 (3-*S*, 3′-*R*), with single hydroxyl group at position 4′, 5′, 6′, or 7′. For each stereoisomer, there were four maximal possibilities regarding the specific positions of hydroxyl group on the phenyl ring. In addition, based on chromatographic peak areas shown in Fig. 2, the first type, i.e., M9, M11, M13, and M15, showed a higher abundance than the second type, i.e., M10, M12, M14, and M16, which suggested that the reduction followed by mono-oxidation metabolism of meisoindigo was regioselective.

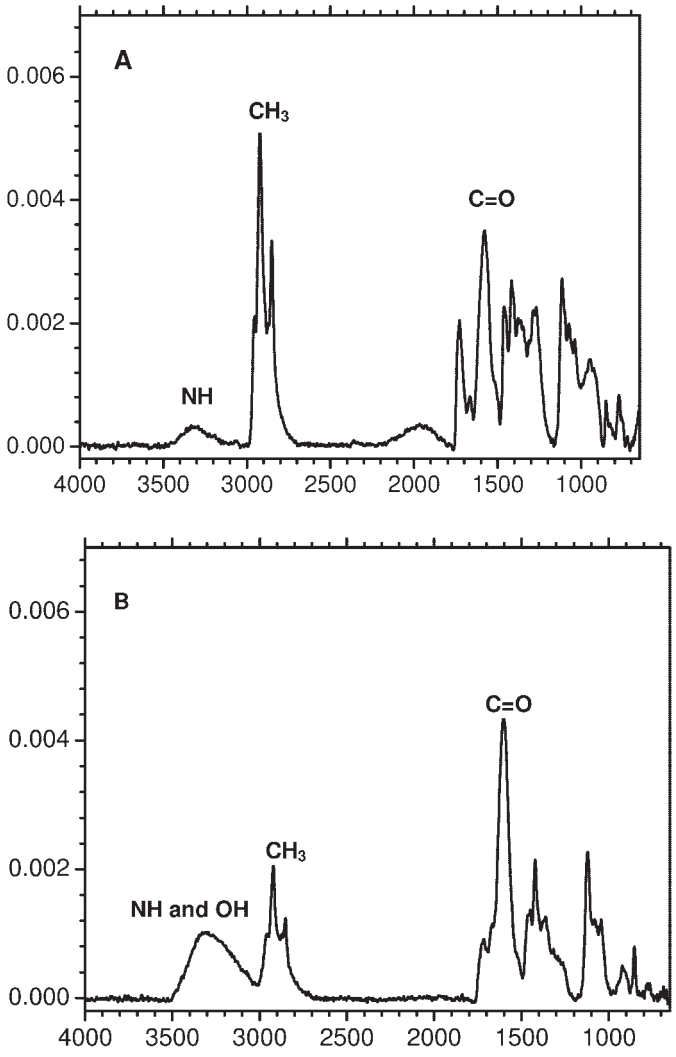

FIG. 8. IR absorption spectra of meisoindigo metabolites at *m/z* 279 (A) and *m/z* 295 (B).

The synchrotron IR absorption spectra of metabolites at *m/z* 295 isolated by analytical HPLC were very similar. The IR spectrum of the most concentrated one was shown in Fig. 8B. The intensity of broad band around 3000 to 3500/cm relative to the band around 2800 to 2900/cm was higher compared with Fig. 8A, indicating the presence of both OH and NH. The OH stretching vibration band was also found to be broad and slightly lower than the NH stretching band. The band around 2800 to 2900/cm was assigned to be CH_3 stretching vibration. The band around 1600/cm was assigned to be C = O stretching vibration. These characteristic absorption bands further confirmed the presence of NH, OH, CH_3, and C = O.

Therefore, M9, M11, M13, and M15 were within the bounds of (3-*R*, 3′-*R*), (3-*S*, 3′-*S*), (3-*R*, 3′-*S*), (3-*S*, 3′-*R*) monohydroxyl reduced-meisoindigo isomers with a single hydroxyl group located at position 4, 5, 6, or 7, whereas M10, M12, M14, and M16 fell within another type of isomers with a single hydroxyl group located at position 4′, 5′, 6′, or 7′.

Incubations under Normoxic and Hypoxic Conditions. The relative percentages of meisoindigo and its metabolites at *m/z* 279 in incubations with rat liver microsomes at various incubation time points are given in Table 4. The results showed that the difference of relative percentages between normoxic and hypoxic incubations was the most significant at 5 min. Approximately 95.81% of meisoindigo, 1.92% of M1+M2, and 2.27% of M3+M4 were found in the 5-min incubation of meisoindigo under normoxic conditions, whereas 66.80% of meisoindigo, 13.12% of M1+M2, and 20.08% of M3+M4 were observed in the 5-min incubation of meisoindigo under hypoxic conditions, thus indicating the occurrence of rapid reductive metabolism of meisoindigo (Table 4). The difference of relative percentages between normoxic and hypoxic incubations attenuated with time until similar relative percentages were found in both normoxic and hypoxic incubations at 60 min (data not shown). As a whole, a quicker onset of the metabolism under hypoxic conditions was obtained as compared with that under normoxic conditions, suggesting oxygen exposure strongly inhibits the in vitro reductive metabolism of meisoindigo in rat liver microsomes.

Discussion

This is the first investigation of the in vitro stereoisomeric metabolites of meisoindigo in rat liver microsomes by achiral and chiral LC/MS/MS, as well as other relevant techniques. In the present study, rat liver microsomes were chosen because rats express two major cytochrome P450 (P450) isoforms that are oligomerically related to human CYP3A4, CYP3A1, and CYP3A2 (Nelson et al., 1996). Besides, rat liver microsomes are readily available though simple preparation. Although the metabolism study in human liver microsomes is not involved yet in this study, the relevant results obtained showed a qualitative similarity in metabolite profiles of meisoindigo between rat liver microsomes and human liver microsomes (data not shown). In addition, the metabolite profile of meisoindigo in rat liver microsomes is more comprehensive than that in human liver microsomes (data not shown). Thus, the findings regarding metabolite profile in rat liver microsomes are of considerable importance.

The abundance of the minor metabolites is generally very low, especially in incubation with low substrate concentration, but is increased relative to other metabolites at higher substrate concentrations. Considering the typical concentration range (10–50 μM) in metabolite identification experiments (Chen et al., 2007), the upper limit concentration, that is, 50 μM, was adopted. Furthermore, minimal sample cleanup was performed because the nature, number, and concentrations of metabolites present were unknown; therefore, it was impossible to determine whether any would be lost during sample preparation (Clarke et al., 2001).

Based on the molecular masses, fragmentation patterns, as well as potential formulae of the metabolites and meisoindigo, three metabolic pathways of meisoindigo in male rat liver microsomes were proposed as direct 3,3′ double-bond reduction, reduction followed by *N*-demethylation, as well as reduction followed by phenyl monooxidation (Fig. 9). Among them, direct 3,3′ double-bond reduction was a one-step reaction and thus the predominant pathway. The other two parallel metabolic pathways were two-step reactions and thus secondary pathways. Interestingly, the first two metabolic pathways of meisoindigo were found to be stereoselective, whereas the third one was both stereoselective and regioselective. In the cases of either M3+M4 versus M1+M2 or M7 (M8) versus M5+M6, the pair of (3-*R*, 3′-*S*) and (3-*S*, 3′-*R*) enantiomers with two hydrogens located at the opposite sides showed a much higher abundance than the other pair of (3-*R*, 3′-*R*) and (3-*S*, 3′-*S*) enantiomers with two hydrogens located at the same sides.

Proton NMR spectroscopy nuclear Overhauser effect (NOE) experiments were conducted to explore the NOE signal difference caused by distinct spatial distance between 3*H* and 3′*H* within the two pairs of synthetic enantiomers, namely, M1+M2 and M3+M4. However, the results showed that there was no significant difference in the NOE spectra between synthetic M1+M2 and M3+M4, when 3*H* and 3′*H*

TABLE 4

Relative percentages of identified components in incubations of meisoindigo with rat liver microsomes under normoxic and hypoxic conditions

Time	Normoxic			Hypoxic		
	Meisoindigo	M1 + M2	M3 + M4	Meisoindigo	M1 + M2	M3 + M4
min	%	%	%	%	%	%
5	95.81	1.92	2.27	66.80	13.12	20.08
15	60.24	15.54	24.23	42.18	21.99	35.83
30	48.30	22.54	29.16	33.48	26.64	39.88

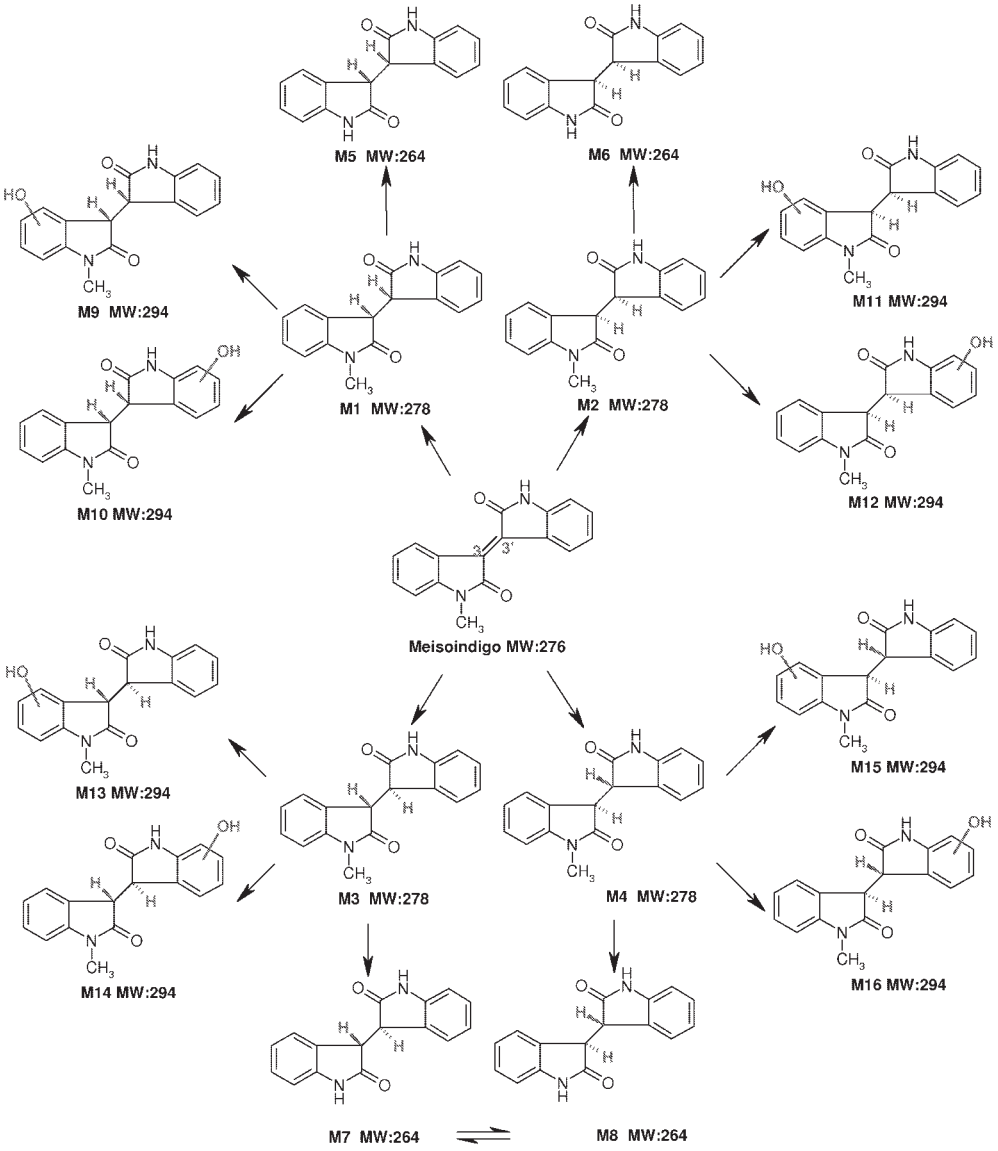

FIG. 9. Proposed metabolic pathway of meisoindigo in rat liver microsomes.

were irradiated, respectively (data not shown). Other methods such as optical rotary dispersion, circular dichroism, or X-ray crystallography could be conducted to confirm the assignment of the absolute configurations of M1+M2 and M3+M4. However, further investigation on the specific absolute configurations of four stereoisomers, i.e., M1, M2, M3, and M4, could be very challenging because of the rapid enantiomer interconversion between M1 and M2 and M3 and M4.

In terms of chiral chromatography analysis, a good separation of metabolite stereoisomers could not be achieved through gradient elution mobile phase, which is typically used for achiral chromatography analysis. Isocratic mobile phase was finally adopted to successfully separate the two pairs of enantiomers at *m/z* 279 simultaneously on a Daicel Chiralcel OD-R column. But this chiral column did not work well on the separation of stereoisomeric metabolites at *m/z* 265 and *m/z* 295, probably owing to their relatively low quantity. Another possible reason might be the specific packing material of Chiralcel OD-R column was only suitable for the chiral separation of stereoisomeric metabolites at *m/z* 279 rather than the other two. In this case, other different types of chiral columns could be considered.

Although the chromatographic peak at *m/z* 295 with retention time of 9.37 min was regarded as the major metabolite, another peak of the pair of enantiomers (M5+M6) with retention time of 9.30 min was

almost coeluted with it (Fig. 2). More sensitive scan-type MRM coupled with UPLC showed that this peak at 9.37 min in Fig. 2 was actually more than one component and combined with three individual peaks showing *m*/*z* 295 (data not shown). Because of the chromatographic complexity and trace amount of these minor metabolites, microsomal incubation samples had been directly tried on the online LC/NMR 600 MHz equipped with a cryoprobe from Bruker BioSpin. Unfortunately, injection volume was limited by the bulk concentration of microsomal matrix contaminants in the first 5 min, which thus diluted the eluted components entering into the NMR detection region. Analytical HPLC was subsequently tried to isolate and accumulate the minor metabolites at *m*/*z* 295 and *m*/*z* 265 for further characterization by 1.7-mm Micro-CryoProbe NMR 600 MHz from Bruker BioSpin. However, the accumulated quantity was still unable to meet the minimal requirement of this special NMR measurement with the lowest detection of limit at present. Therefore, chemical synthesis has to be the last resort. Further work would be needed to synthesize the possible minor metabolites and isolate the stereoisomers by chiral chromatography followed by NMR structural characterization. In particular, the specific position of the OH group in stereoisomeric monohydroxyl reduced meisoindigo is a vital aspect to be investigated. Because both NCH3 at position 8 and NH at position 8′ donate electrons into the two phenyl ring systems, the highest electron density should be located at *ortho* positions (i.e., 7 or 7′) and *para* positions (i.e., 5 or 5′). In view of the offset by steric hindrance of the OH group at *ortho* positions, it could be predicted that *para* positions (i.e., 5 or 5′) would be thus the most reactive toward perferryl oxygen complex $[FeO]^{3+}$ from the perspective of P450 oxidation mechanism.

Considering synchrotron IR spectroscopy provided a much greater detection of limit than conventional IR technique because of the high brightness of synchrotron IR source, it was used for the first time to further confirm the structures of metabolite within the milligram level after isolation and accumulation by analytical HPLC. The IR measurement was performed in the vacuum to remove the signals caused by H_2O and CO_2 from the air as much as possible, thus achieving a satisfactory signal/noise ratio. It should be noted that synchrotron IR is only applicable for those limited instances in which the structural difference between metabolite and parent drug is characteristic IR functional groups, such as hydroxyl group, carbonyl group, amino group, and so on. Hence, synchrotron IR can only be a supplementary tool to conventional structural identification approaches, that is, MS and NMR.

The comparative metabolite profiling using rat liver microsomes in the normoxic and hypoxic incubations further confirmed the occurrence of reductive metabolism of meisoindigo. Based on a report on the reductive metabolism of meisoindigo analogs (Kohno et al., 2005), it is possible to speculate that NADPH/P450 reductase in rat liver microsomes could be the enzyme responsible for the initiation of reductive activation of meisoindigo through the formation of a superoxide radical by transferring one electron from the electron donor, that is, NADPH. This proposed mechanism can be confirmed by investigating the metabolism of meisoindigo after incubation with purified recombinant P450 reductase in the presence of NADPH.

Acknowledgments. We thank Dr. Mohammed Bahou from Singapore Synchrotron Light Source, National University of Singapore, for assistance with synchrotron IR experiments.

References

Bradford MM (1976) A rapid and sensitive method for the quantitation of microgram quantities of protein utilizing the principle of protein-dye binding. *Anal Biochem* **72:**248–254.
Chen Y, Monshouwer M, and Fitch WL (2007) Analytical tools and approaches for metabolite identification in early drug discovery. *Pharm Res* **24:**248–257.
Clarke NJ, Rindgen D, Korfmacher WA, and Cox KA (2001) Systematic LC/MS metabolite identification in drug discovery. *Anal Chem* **73:**430A–439A.
Cooperative Group of Clinical Therapy of Meisoindigo (1988) Clinical studies of meisoindigo in the treatment of 134 patients with CML. *Chin J Hematol* **9:**135–137.
Cooperative Group of Phase III Clinical Trial on Meisoindigo (1997) Phase III clinical trial on meisoindigo in the treatment of chronic myelogenous leukemia. *Chin J Hematol* **18:**69–72.
Gibson GG and Skett P (1994) Techniques and experiments illustrating drug metabolism, in *Introduction to Drug Metabolism* (Gibson GG and Skett P eds) pp 240–242, Blackie Academic and Professional, London.
Kohno Y, Kitamura S, Yamada T, Sugihara K, and Ohta S (2005) Production of superoxide radical in reductive metabolism of a synthetic food-coloring agent, indigocarmine, and related compounds. *Life Sci* **77:**601–614.
Kostiainen R, Kotiaho T, Kuuranne T, and Auriola S (2003) Liquid chromatography/atmospheric pressure ionization-mass spectrometry in drug metabolism studies. *J Mass Spectrom* **38:**357–372.
Liu BC, Qian LS, Wang Y, Xiao ZJ, Han JL, Li X, Zhou Z, and Liu YH (2000) The clinical effect and mechanism of meisoindigo in chronic granulocytic leukemia. *Chin J Prac Intern Med* **20:**610–612.
Nelson DR, Koymans L, Kamataki T, Stegeman JJ, Feyereisen R, Waxman DJ, Waterman MR, Gotoh O, Coon MJ, Estabrook RW, et al. (1996) P450 superfamily: update on new sequences, gene mapping, accession numbers and nomenclature. *Pharmacogenetics* **6:**1–42.
Peng Y and Wang MZ (1990) Screening for in vitro metabolites of meisoindigo using RP-HPLC-DAD with gradient elution. *Acta Pharmaceutica Sinica* **25:**208–214.
Prakash C, Shaffer CL, and Nedderman A (2007) Analytical strategies for identifying drug metabolites. *Mass Spectrom Rev* **26:**340–369.
Xiao Z, Hao Y, Liu B, and Qian L (2002) Indirubin and meisoindigo in the treatment of chronic myelogenous leukemia in China. *Leuk Lymphoma* **43:**1763–1768.
Xiao Z, Qian L, Liu B, and Hao Y (2000) Meisoindigo for the treatment of chronic myelogenous leukemia. *Br J Haematol* **111:**711–712.
Xiao Z, Wang Y, Lu L, Li Z, Peng Z, Han Z, and Hao Y (2006) Anti-angiogenesis effects of meisoindigo on chronic myelogenous leukemia in vitro. *Leuk Res* **30:**54–59.

Address correspondence to: Paul C. Ho, Department of Pharmacy, National University of Singapore, 18 Science Drive 4, Singapore 117543. E-mail: phahocl@nus.edu.sg